Modafinil Alters Intrinsic Functional Connectivity of the Right Posterior Insula: A Pharmacological Resting State fMRI Study

Nicoletta Cera[1], Armando Tartaro[1], Stefano L. Sensi[1,2,3]*

1 Department of Neuroscience and Imaging, University "G. d'Annunzio" Chieti-Pescara, Chieti, Italy, **2** Molecular Neurology Unit, Center of Excellence on Aging, University "G. d'Annunzio", Chieti-Pescara, Chieti, Italy, **3** Departments of Neurology and Pharmacology, Institute for Memory Impairments and Neurological Disorders, University of California-Irvine, Irvine, CA, United States of America

Abstract

Background: Modafinil is employed for the treatment of narcolepsy and has also been, off-label, used to treat cognitive dysfunction in neuropsychiatric disorders. In a previous study, we have reported that single dose administration of modafinil in healthy young subjects enhances fluid reasoning and affects resting state activity in the Fronto Parietal Control (FPC) and Dorsal Attention (DAN) networks. No changes were found in the Salience Network (SN), a surprising result as the network is involved in the modulation of emotional and fluid reasoning. The insula is crucial hub of the SN and functionally divided in anterior and posterior subregions.

Methodology: Using a seed-based approach, we have now analyzed effects of modafinil on the functional connectivity (FC) of insular subregions.

Principal Findings: Analysis of FC with resting state fMRI (rs-FMRI) revealed increased FC between the right posterior insula and the putamen, the superior frontal gyrus and the anterior cingulate cortex in the modafinil-treated group.

Conclusions: Modafinil is considered a putative cognitive enhancer. The rs-fMRI modifications that we have found are consistent with the drug cognitive enhancing properties and indicate subregional targets of action.

Trial Registration: ClinicalTrials.gov NCT01684306

Introduction

Modafinil is a compound employed in the treatment of sleep disorders, and, off-label, also used for the treatment of cognitive deficits in schizophrenia, Attention Deficit/Hyperactivity Disorder (ADHD), and mood disorders [1–5]. Previous preclinical and human studies have indicated that modafinil modulates neuro-transmission in several brain regions including the hypothalamus, hippocampus, basal ganglia and prefrontal regions. The compound acts on orexin, monoamines and dopamine as well as on glutamate, and gamma-aminobutyric acid [6–8]. Recent studies have indicated that modafinil positively modulates attention, memory, and executive functions [9,10]. Modafinil can be considered a cognitive enhancer that, compared to amphetamine-like psychostimulants, may have lower risks of inducing addiction [11–13].

In a previous study, we have reported that the administration of a single dose (100 mg) of modafinil affects the brain resting state network (RSN) activity in healthy young individuals [14]. The study showed that, of six selected RSNs [the Default Mode Network, the Salience Network (SN), the Fronto Parietal Control network (FPC; lateralized in both hemispheres), the Sensory Motor Network, the Exstrastriate Visual System and the Dorsal Attention Network (DAN)], functional connectivity (FC) effects were found only in the FPC and DAN. No statistically significant modifications were observed in the SN.

The SN is composed of three nodes. The SN includes the bilateral insular cortices and dorsal anterior cingulate cortex as well as subcortical structures like the amygdala, the substantia nigra/ventral tegmental area, and the thalamus [15]. The SN plays an important role in controlling attention toward biologically-relevant and cognitively-relevant stimuli present in the
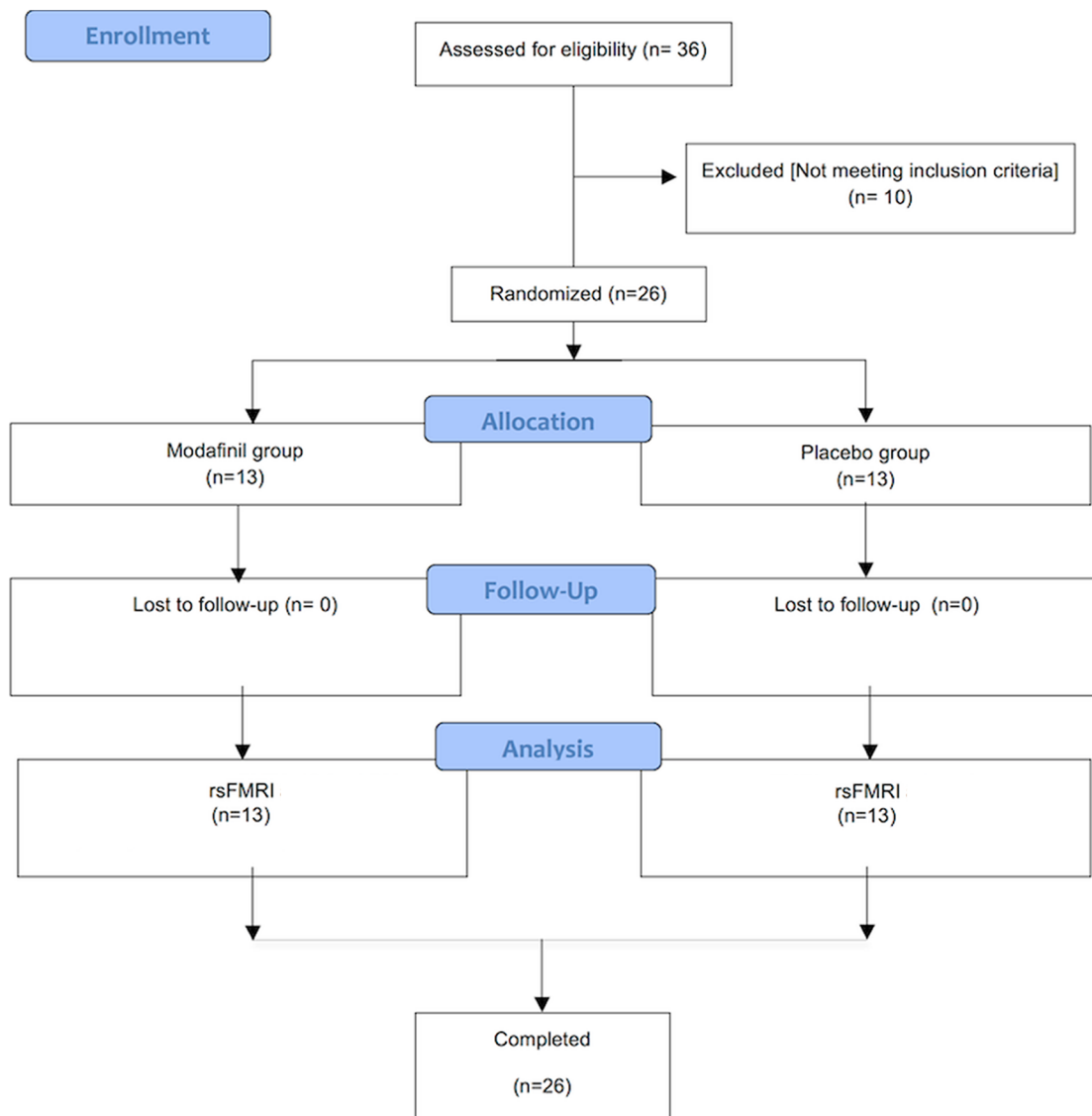
Figure 1. CONSORT Diagram. Flow diagram graphically describes the design of the study: enrollment, intervention, follow-up and data analysis.
doi:10.1371/journal.pone.0107145.g001

environment [15,16], an overall function that helps to guide behavior.

Several imaging studies have shown that the insula and cingulate cortex are simultaneously activated upon cognitive tasks [17]. The insula is indeed considered a critical hub that mediates the information flow within the SN [15,16]. The region interacts with limbic, somatosensory, and motor regions and is also crucial in the coordination of sensorimotor, visceral, and interoceptive processing as well as in controlling homeostatic/allostatic functions like self-awareness and empathy [18–20]. The insula is also critical in controlling motivation, a process that is partly mediated by the activation of the orexin receptor, a preferential pharmacological target for modafinil [21]. In summary, functioning of the insula is important in the response to salient environmental stimuli as the region promotes a spatio-temporal integration that is needed for cognitive and emotional elaborations [16].

Several studies have shown functional sub-differentiations within the insular cortex when considering the activity of the anterior versus posterior portions of the region. The anterior part

appears to be mainly involved in cognitive and socio-cognitive functions such as empathy processing, emotional salience detection, and attentional control [15;22–24]. The posterior part modulates sensorimotor tasks [25]. These different functions are matched by distinct connectivity patterns between the two subregions and other brain areas. The anterior insula is functionally connected with the Anterior Cingulate Cortex (ACC) whereas the posterior insula appears to be mainly connected with the somatosensory and middle cingulate cortices [16,17,26].

In a previous study, we have observed that healthy young individuals, after modafinil administration, showed improvement in fluid reasoning as measured with Advanced Progressive Matrices (APM) [14,27]. Previous imaging studies have indicated that SN nodes, i.e.: bilateral insulae and the cingulate cortex are involved in tasks set to stimulate fluid reasoning [28,29] but in our study were unable to detect significant modafinil effects on SN activation [14]. In the past decade, resting state fMRI (rs-fMRI) has emerged as valuable tool for the study of neural activity when

Table 1. Between-group comparison for right posterior insula for the contrast T1>T0.

Cluster	BA	Hemisphere	X	Y	Z	Nr. Voxels
SFG	6	R	55.3	−4.1	23.1	60
MTG	22	R	46.9	−407.	15.8	1053
Putamen		R	27.8	9	1.1	197
Precuneus	29/30	R	18.1	−55.9	28.5	159
ACC	24	R	10.2	−20	31.5	317
SFG	6	R	0.6	−13.9	55.4	2643
dorsal PCC	31	R	2.7	−20	37.9	137
ACC	24	L	−12.7	−2.9	31.7	855
Putamen		L	−22.8	1	−4.7	118
Posterior Insula/temporal pole	13/38/34	L	−45.4	−4	−0.1	2836
Anterior prefrontal cortex	10	L	−33.2	26.9	20.2	68

Table indicates brain regions showing significant differences when considering T1 (drug >placebo)>T0 (drug>placebo) for the right Posterior Insula (PIrh). Brain regions are listed with the mean Talairach coordinates (x: left-right; y: anterior-posterior; z: dorsal ventral) and the corresponding number of voxels.
Abbreviations: BA: Brodmann's area; L: left; R: right. PCC: Posterior Cingulate Cortex; MTG: Middle Temporal gyrus; ACC: Anterior Cingulate cortex; SFG: Superior Frontal gyrus.
doi:10.1371/journal.pone.0107145.t001

the brain is at rest and not involved in task completion. Compared to task-related fMRI, rs-fMRI offers the advantage of allowing the investigation of simultaneous and coordinated activity of multiple and well-defined brain networks. This approach also reduces confounding factors like the inter-individual variability in task compliance and/or performance that can occur upon fMRI acquisition [14]. rs-fMRI has been successfully employed to evaluate FC modifications [30]. FC is studied with MRI through the analysis of simultaneous variations of BOLD (Blood-Oxygen-Level-Dependent) signals occurring in distinct brain regions [24,31,32]. FC can be studied at rest by evaluating spontaneous low frequency fluctuations of BOLD signals in different brain voxels. The process allows the identification of temporally-related patterns of activity across brain regions that are involved in similar or related functions [33].

Given the subregional differentiation of the insular cortex and its role in the SN, we have decided to re-analyze our fMRI data with the aim of exploring modafinil-induced subregional patterns of FC that is occurring within the insulae as these insular subregions are central for the beneficial cognitive effects we have observed after a single dose exposure to the drug [14].

To that aim, fMRI acquisitions obtained in the previous study were now analyzed with a seed-based approach that was focused only on activity occurring in the left and right insulae divided in anterior and posterior subregions.

Materials and Methods

Ethics Statement

The protocol for this trial and supporting CONSORT checklist are available as supporting information; see Checklist S1 and Protocol S1.

The study was approved by the ethics committee of University of Chieti (PROT 2008/09 COET on 14/10/2009) and conducted in accordance with the Helsinki Declaration.

The study design was explained in detail and written informed consent was obtained from all participants involved in our study. Recruitment was performed throughout February 2011, drug/placebo administration and fMRI acquisitions started on March 2011, went on until January 2102, and the study was completed

with the last fMRI session in January 2012. After securing financial coverage for costs related to the analysis of the study, the trial was registered on 10/09/2012 (ClinicalTrials.gov NCT01684306 http://clinicaltrials.gov/ct2/show/NCT01684306). After obtaining registration, the double blind study was opened and analyzed, rs-fMRI data were investigated by means of independent component analysis (ICA) leading to a first publication of the dataset[14]. The protocol is the same as the previous study [14] with no deviations made. The authors confirm that all ongoing and related trials for these drug/interventions are registered.

Study group, design, and rs-fMRI acquisition

The study group, experimental design, and rs-fMRI data acquisition are described in the original study [14; Figure 1]. Randomization of study subjects was obtained by means of random number generator. In our study, in line with similar pharmacological-fMRI studies, and also considering that we did not have preliminary data that could be used to, a priori, estimate the optimal sample size, we have evaluated two groups of 13 subjects that is nowadays an accepted size in these kind of studies.

MRI/fMRI data analysis

MRI and fMRI data were analyzed with the Brain Voyager QX 2.3 software (Brain Innovation, Maastricht, The Netherlands). Preprocessing of functional data was performed by sequentially applying slice scan time correction, three-dimensional motion correction, and removal of linear trends from voxel time series. Preprocessed functional volumes were then co-registered with the corresponding structural dataset. Both structural and functional volumes were then transformed into the Talairach space [34] using a piecewise affine and continuous transformation. Functional volumes were re-sampled at a voxel size of $3 \times 3 \times 3$ mm^3. A spatial smoothing with a Gaussian kernel of 6.0 mm full-width half-maximum was applied to functional images corresponding to two voxels in the re-sampled data to account for intersubject variability while maintaining a relatively high spatial resolution.

FC analysis

Previous studies have identified different subregions in the insular cortices in both humans and non-human primates [35].
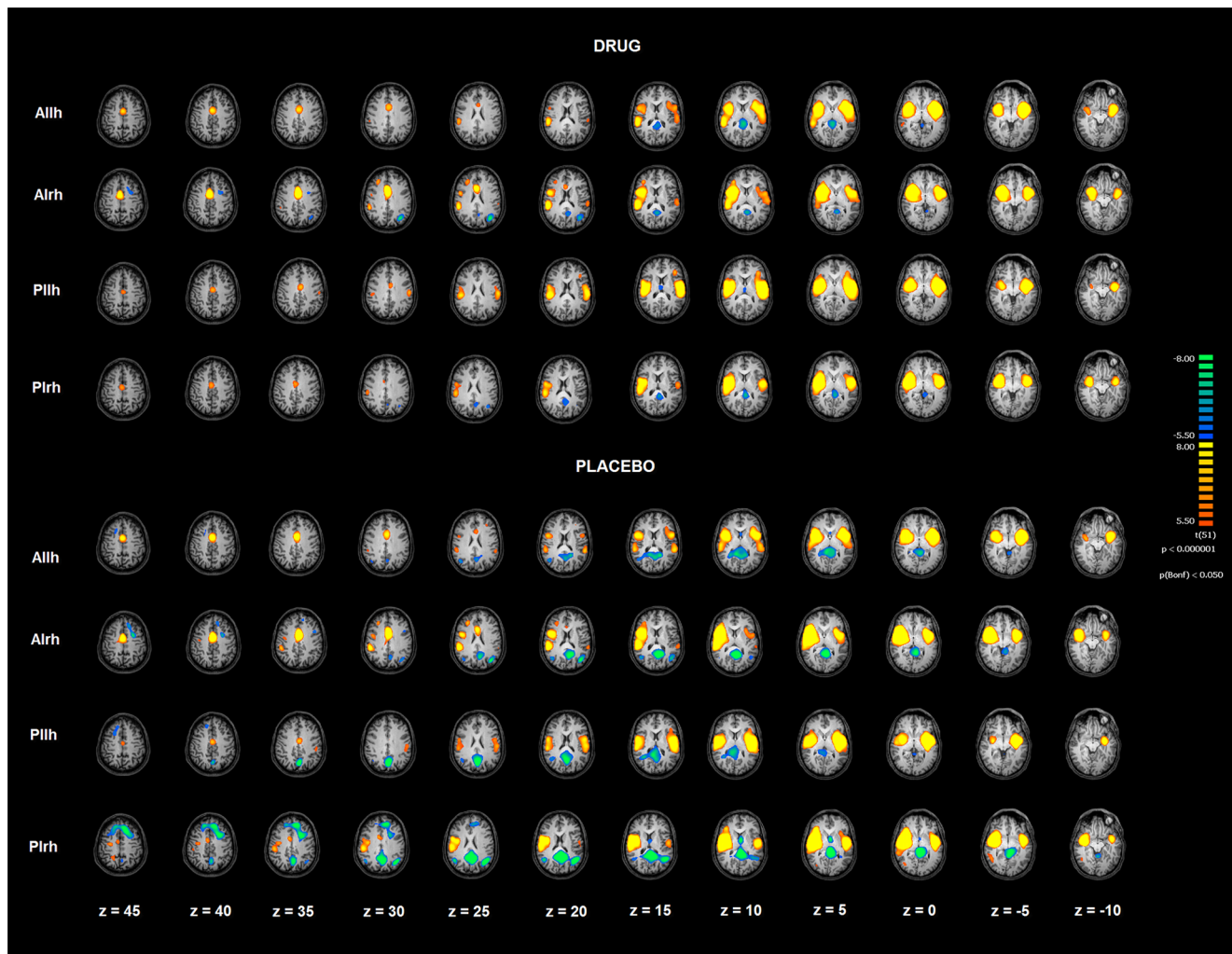
Figure 2. Insula functional connectivity patterns before drug/placebo treatment. Image depicts functional connectivity patterns of the four subregions of bilateral insulae as assessed with rs-fMRI. Maps are overimposed on a Talairach atlas and in radiological convention with a statistical significance set at p<0.05 Bonferroni corrected. AIlh = anterior insula left hemisphere; AIrh = anterior insula right hemphere; PIlh = posterior insula left hemisphere; PIrh = posterior insula right hemisphere.
doi:10.1371/journal.pone.0107145.g002

These subregions appear to show different connectivity patterns with remaining brain regions. To examine FC patterns in the insular cortices, four ROIs were selected for each subject, before and after drug/placebo administrations, within the anterior portion of the left hemisphere (AIlh) or right hemisphere (AIrh) and posterior portions of the left (PIlh) or right hemisphere (PIrh). Regions of interest (ROIs) were determined using Talairach coordinates. Talairach coordinates are defined on the basis of two brain structures: the anterior and posterior commissures. Distances in Talairach coordinates are measured from the anterior commissure that is, by convention, intended as the origin [34]. The y-axis represents the anterior

->posterior direction, the x-axis represents the left->right, and the z-axis is depicts the dorsal->ventral direction (Table 1, [34]). Each ROI was created by means of TalCoord2VOI plug-in with a radius of 2,5 mm to avoid White Matter (WM) inclusions.

Whole brain seed-based connectivity maps, related to the selected ROIs (see above), were created for all subjects. We then calculated correlations between ROI time-courses (i.e.: the time-course in each of the insula subregions) and all the time-courses of

the brain voxels [36]. BOLD time-courses were extracted from each ROI by obtaining an average value for each voxel of the ROI modeled for each single subject. To reveal FC patterns that were consistent for the groups along with the T0 and T1 time points in relation to each insular subregions, we proceeded in the following way: after applying the Fisher's r-to-z transformation to each correlation map, random-effect analysis was independently performed for each of the two study groups and the two acquisition time points.

FC maps were computed according to Margulies et al. [37]. Nuisance covariates were included in the analyses to reduce effects of physiological processes such as fluctuations related to cardiac and respiratory cycles [38,39] or to motion. To this aim, we included eight additional covariates that modeled nuisance signals sampled from WM and Cerebro-Spinal Fluid (CSF) [40], as well as from six motion parameters (3 rotations and 3 translations as saved by the 3D motion correction). We derived WM/CSF nuisance signals averaging voxel time courses in each subject whole brain WM/CSF masks. These masks were generated by the segmentation process of each subject brain by means of Brain
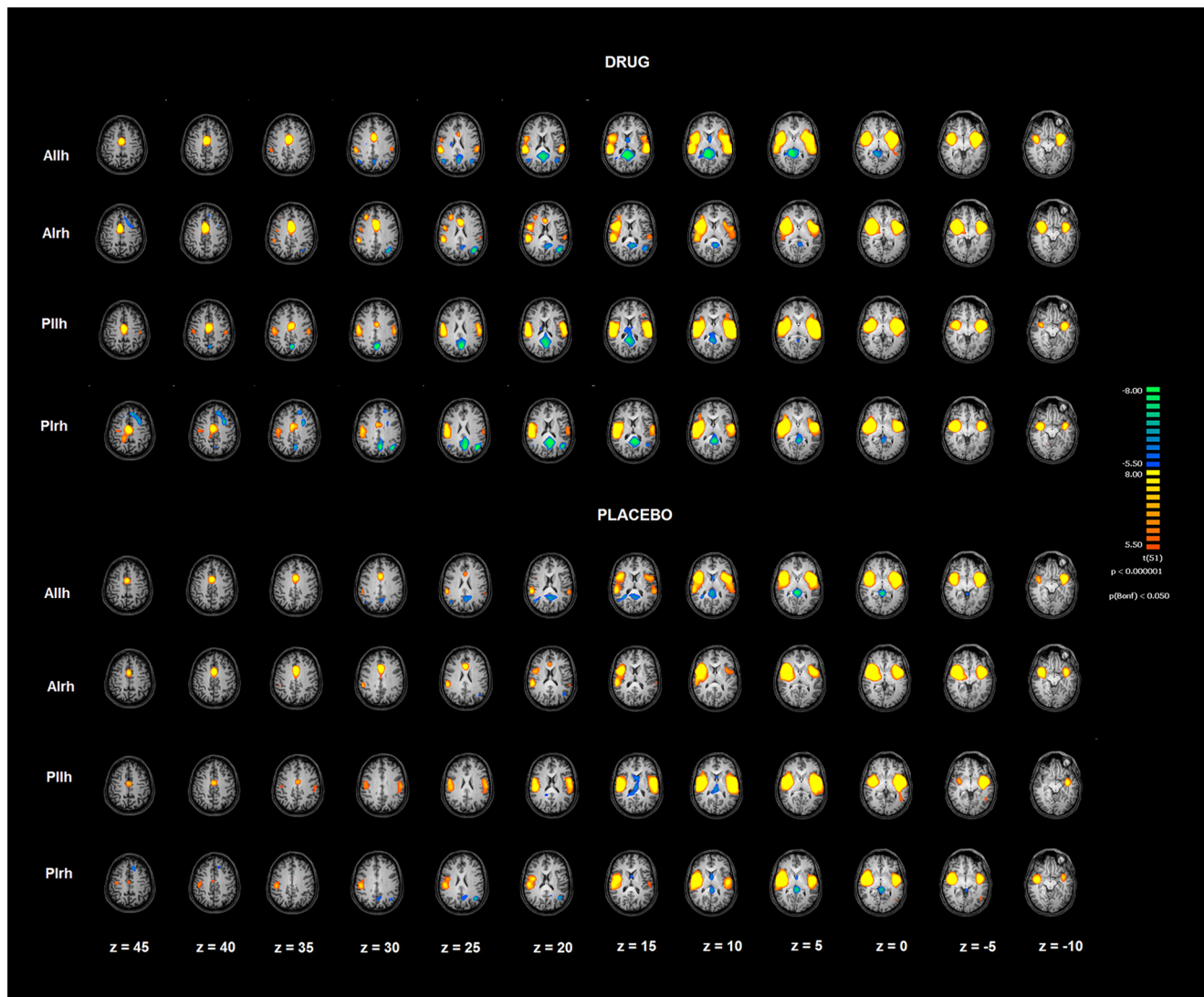
Figure 3. Between-group comparison of the right posterior insula pattern before and after drug/placebo treatment. Image depicts the map obtained after contrast T1 (drug>placebo) >T0 (drug>placebo) for the right posterior insula (PIrh). The map is overimposed on a Talairach atlas and in radiological convention (p<0.02 FDR corrected). Differences are assessed by means of a mixed model voxel wise ANOVA with a between-group factor (Drug vs Placebo) and a repeated measure factor (T0 vs. T1).
doi:10.1371/journal.pone.0107145.g003

voyager QX. All seed-based predictors were z-normalized and analyses repeated with each insular subdivision inserted in a separate regression model.

Statistical analysis

For each seed ROI, subject, and condition (drug vs. placebo), and time (T0 vs. T1), a FC map was computed on a voxel-wise basis. For each subject, the general linear model (GLM) [41] for multiple regression analysis produced four ROI-based t-maps. To assess group differences between T0 and T1, four different voxel-wise mixed model Analyses of Variances were performed by means of the ANOVA tool of Brain Voyager QX set with one between-group factor (drug vs. placebo) and a repeated measure factor (T1 vs. T0). To control for absence of between-group differences, a between-group comparison was performed at T0. To assess effect of drug/placebo network FC of each ROI, we performed the contrast T1 (drug>placebo)> T0 (drug>placebo). Statistical significance was assessed by setting a threshold that was

corrected by the False Discovery Rate (FDR) [q<0.02 corresponding to t>3.93 and p<0.001 at voxel level; 42]. To avoid circularity effects, statistical analyses were performed in accordance with what indicated by Kriegerskorte and colleagues [43].

Results

Four patterns of ROI seed-based FC patterns were investigated in specific insular subdivisions. The analysis was performed on rs-FMRI data at T0 (before the administration of drug/placebo) and T1 (after the administration of drug/placebo). FC maps were calculated for each seed ROI [Anterior Insula left hemisphere (AIlh); Anterior Insula right hemisphere (AIrh); Posterior Insula left hemisphere (PIlh); Posterior Insula right hemisphere (PIrh)] and showed distinct patterns of connectivity in specific insular subregions. Resulting maps were corrected for multiple comparisons by means of Bonferroni correction with a threshold set at p< 0.05 (Figure 2 and 3, Table 2). At T0, no differences were found

Table 2. Insula subregional seed-based correlation.

Anterior insula - Left hemisphere	Seed: x = −38; y = 15; z = −2						
Cluster	BA	Hemisphere	X	Y	Z	Nr. Voxels	
T0 -Drug							
Insula IFG pars opercularis and triangularis	13/44/45						
STG putamen	/22/41	R	43.2	−6.7	5.9	44739	
Parahippocampus temporal pole amygdala		R	30.9	−28.2	−20.5	186	
Retrosplenial PCC	29/31	L	−0.2	−39.1	9.1	8517	
Ventral and dorsal ACC premotor cortex	24/32/6	R	11	0.2	40.8	10995	
Insula IFG pars opercularis and triangularis	13/44/45						
STG putamen	/22/41	L	−41.3	0.5	2.6	49422	
T0 - Placebo							
Insula IFG pars opercularis and triangularis	13/22/44						
STGputamen	/45/41	R	41.8	−1.9	6	42945	
Retrosplenial PCC	23/29/31	R	4.5	−47.8	11.1	29163	
Parahippocampus temporal pole amygdala	38	R	30.1	−24.5	−16.5	1091	
MFG	8	R	20.7	16.7	43.3	685	
Ventral and dorsal ACC premotor cortex	32/24/6	L	−0.1	1.2	39.4	13217	
Insula IFG pars opercularis and triangularis	13/22/44						
STG putamen	/45/41	L	−42.5	−0.9	3.5	47833	
Dorsolateral preforntal cortex	9	L	−31.5	36.2	24.4	284	
T1 - Drug							
Insula IFG pars opercularis and triangularis							
STG putamen	44/47/13/40	R	43.9	−7.7	7.9	51049	
Retrosplenial PCC	30/31/23	R	4.2	−47.2	13.5	28483	
Parahippocampus temporal pole amygdala	38	R	30.5	−26.8	−19.1	334	
Extra striate cortex	18	R	23.8	−78.5	−18.5	523	
Cudate Nucleus		R	20.8	−12.9	25.5	496	
Ventral and dorsal ACC premotor cortex	6/24/32	R	0	−2.7	40.6	16971	
MFG	8	L	−13.1	31.9	40	65	
Insula IFG pars opercularis and triangularis	13/45/44						
STGputamen	/41/42/22	L	−44.4	−6.6	4.1	57332	
Augular and supramerginal gyrus	39/40	L	−42.1	−64	23.3	1865	
T1 - Placebo							
Insula IFG pars opercularis and triangularis	44/45/13						
STG putamen	/22/40/41	R	43.1	−1.9	6.2	42772	
Retrosplenial PCC	30/29/23/31	R	5.4	−46.9	13.2	18684	
Ventral and dorsal ACC premotor cortex	6/24/32	R	0.5	2.7	38.8	11655	
Insula IFG pars opercularis and triangularis	44/45/13						
STG putamen	/22/40/41	L	−42.2	−1.1	3.1	43055	
Anterior insula - Right hemisphere	Seed: x = 37; y = 16; z = 3						
Cluster	BA	Hemisphere	X	Y	Z	Nr. Voxels	
T0 - Drug							
Insula IFG pars opercularis and triangularis	13/22/44/45/4						
STGputamen thalamus	1	R	39.8	−2.0	6.6	70971	
Ventral and dorsal ACC	32/24	R	3.2	0.3	40	23859	
PCC	30	L	−2.9	−52.5	12.3	5600	
SFG/MFG	6/8	L	−26.7	6.3	42.3	2167	
Insula IFG pars opercularis and triangularis	13/22/44/45/4						
STGputamen thalamus	1	L	−43.4	−1.4	2	30606	
	39	L	−36.6	−66.9	25.4	5522	

Table 2. Cont.

Anterior insula - Right hemisphere	Seed: x = 37; y = 16; z = 3						
Cluster	BA	Hemisphere	X	Y	Z	Nr. Voxels	
T0 - Placebo							
Insula IFG pars opercularis and triangularis	13/22/44/45/4						
STGputamen thalamus	1	R	41.1	−3.5	7.9	84229	
Angular and supramarginal gyrus	39/40	R	42.8	−65.7	18.7	1862	
Ventral and dorsal ACC	32/24	R	3.9	−2.9	40.5	24955	
Retrosplenial PCC	23/30/31	L	−5.2	−51.2	11.2	24438	
SFG/MFG	6/8	L	−20.3	16.4	45	6172	
Parahippocampus temporal pole amygdala		L	−27.8	−17.2	−22.3	1174	
Insula IFG pars opercularis and triangularis	13/22/44/45/4						
STGputamen thalamus	1	L	−40.9	2	−0.3	23190	
Angular and Supramarginal gyrus	39/40	L	−40.6	−66.9	20.1	5946	
SFG premotor cortex	6	L	−44.2	10.2	33.6	537	
STG	22/42	L	−60.1	−32.7	16.3	1413	
T1 - Drug							
Insula IFG pars opercularis and triangularis	13/22/44/45/4						
STGputamen thalamus	1	R	39.5	−0.9	7.7	71046	
Ventral and dorsal ACC	32/24	R	1.7	2.6	38.0	24485	
Retrosplenial PCC	23/30/31	L	−5.4	−52.2	14.7	7612	
SFG premotor cortex	6	L	−21.9	16.8	44.7	2611	
Insula IFG pars opercularis and triangularis	13/22/44/45/4						
STGputamen thalamus	1	L	−42	−1.5	1.7	31194	
Angular and supramarginal gyrus	39/40	L	−40.5	−64.2	23.2	6336	
T1 - Placebo							
Insula IFG pars opercularis and triangularis	13/22/44/45/4						
STGputamen thalamus	1	R	40	−2	5.3	59401	
Ventral and dorsal ACC	32/24	R	1.4	7.4	35.5	16035	
Insula IFG pars opercularis and triangularis	13/22/44/45/4						
STGputamen thalamus	1	L	−38.0	3.7	−0.7	23429	
Angular and Supramarginal gyrus	39/40	L	−41.7	−63.4	20.6	825	
STG	22/42	L	−59.4	−33.5	18.5	382	
Posterior insula – Left hemisphere	seed: x = −42; y = −9; z = 4						
Cluster	BA	Hemisphere	X	Y	Z	Nr. Voxels	
T0 – Drug							
Insula IFG pars opercularis and triangularis	13/22/44						
STG putamen	/45/41	R	43.9	−8.9	8.8	44235	
ACC	24	L	−0.5	−6.9	37.5	4060	
	13/22/44/						
Insula IFG pars opercularis and triangularis pre and post central gyrus STG putamen	45/41/2/4/3/6	L	−44.7	−8	6.7	62929	
T0 – Placebo							
Insula IFG pars opercularis and triangularis	13/22/						
STG putamen	44/45/41	R	43.7	−7.6	9.3	36180	
PCC SPL	23/30/31/7	R	6	−52.4	18.9	33283	
MFG	8	R	20	23.8	44.5	2378	
ACC	24	L	−1.4	−8.2	38.2	3288	
	13/22/44/						
Insula IFG pars opercularis and triangularis pre and post central gyrus STG putamen	45/41/2/4/3/6	L	−43.6	−8.7	7.7	58956	

Table 2. Cont.

Posterior insula – Left hemisphere	seed: x = −42; y = −9; z = 4						
Cluster	BA	Hemisphere	X	Y	Z	Nr. Voxels	
T1 – Drug							
Insula IFG pars opercularis and triangularis pre and post central gyrus STGputamen	13/22/44/45/41/2/3/3/6	R	44.7	−10.2	11	54610	
PCC SPL	23/30/31/7	L	−0.4	−49.8	20.2	22724	
ACC	24	R	0.1	−11.5	42.3	14520	
Insula IFG pars opercularis and triangularis pre and post central gyrus STGputamen	13/22/44/45/41/2/4/3/6	L	−46.5	−9.4	8.2	64141	
Angular gyrus	39	L	−43.2	−63.7	22.3	64	
T1 – Placebo							
Insula IFG pars opercularis and triangularis	13/22/44/						
STG putamen	45/41	R	45.2	−7.9	11.2	42828	
ACC	24	R	0.5	−8.9	42.1	5533	
Insula IFG pars opercularis and triangularis pre and post central gyrus STGputamen	13/22/44/45/41/2/4/3/6	L	−45.5	−11.1	8.3	59758	
Posterior insula - Right hemisphere	seed: x = 39; y = −9; z = 9						
Cluster	BA	Hemisphere	X	Y	Z	Nr. Voxels	
T0 - Drug							
Insula IFG pars opercularis and triangularis	13/22/44/						
STG putamen	45/41	R	43.4	−7.6	6.3	55307	
SPL	7	R	18.3	−48.1	51.8	122	
SFG ventral and dorsal ACC	6/32/24	R	4.8	−10.1	44.6	6387	
PCC	23/30/31	L	−3.9	−44.2	12.2	8458	
Insula IFG pars opercularis and triangularis	13/22/44/						
STG putamen	45/41	L	−44.9	−3.7	1.2	26362	
Angular gyrus	39	L	−38.7	−65.1	25.5	728	
T0 - Placebo							
Insula IFG pars opercularis and triangularis	13/22/24 44/						
ACC STG putamen	45/41	R	40.8	−7.6	10.6	91610	
PCC angular gyrus	23/30/31	L	−11.1	−46.8	15.4	67270	
Prefrontal cortex	8/10	L	−9.7	25.7	40.3	37524	
Angular gyrus	39	R	−44.2	−59.6	22.6	3245	
Insula IFG pars opercularis and triangularis	13/22/44/						
STG putamen	45/41	L	−46.8	−6.5	0.8	25923	
SPL	7	R	19.7	−52.7	4.8	1229	
T1 - Drug							
Insula IFG pars opercularis and triangularis	13/22/44/						
STG putamen	45/41	R	43.4	−9.1	10	65731	
ACC SFG pre and postcentral gyrus	24/6/1/2/3	R	6.8	−19.2	46.2	25291	
PCC	23/30/31	L	−3.2	−51.4	18	24282	
Dorsolateral prefrontal cortex	9	L	−20.6	22.1	40.9	10736	
Insula IFG pars opercularis and triangularis	13/22/44/						
STG putamen	45/41	L	−47.6	−6.7	4.1	29616	
Angular gyrus	39	L	−42	−63.7	24.1	5383	
Angular gyrus	39	R	45.4	−62.6	23.2	254	
T1 - Placebo							
Insula IFG pars opercularis and triangularis	13/22/44/45/41/6/3/4/						
STGputamen pre and postcentral gyrus	2	R	43.9	−8.9	9.7	58139	
SPL	7	R	20.9	−47.1	51.9	1826	
Caudate nucleus		R	13.7	22.2	11.6	436	

Table 2. Cont.

Posterior insula - Right hemisphere	seed: x = 39; y = −9; z = 9					
Cluster	BA	Hemisphere	X	Y	Z	Nr. Voxels
SFG ACC	24/6	R	4.8	−15.4	47.8	1741
Precuneus	29	L	−5.9	−59.8	26	2072
PCC	23/29	L	−2.5	−36.1	4.2	5523
MFG	8	L	−12	26.6	46.4	1861
SPL	7	L	−24.1	−41.7	54.9	321
Insula IFG pars opercularis and triangularis	13/22/44/45/					
STG putamen	41	L	−46.8	−8.2	1.9	21263
Angular gyrus	39	L	−41	−61.9	23.5	2094

Table indicates brain regions showing seed-based functional connectivity [with significance level set at P<0.05 (Bonferroni corrected)] for the left anterior (AIlh) right anterior (AIRh) left posterior (PIlh) and right posterior (PIrh) at T0 or T1 respectively. Brain regions are listed according to mean Talairach coordinates (x: left-right; y: anterior-posterior; z: dorsal ventral) and corresponding number of voxels.
Abbreviations: BA: Brodmann's area; L: left; R: right. PCC: Posterior Cingulate Cortex; MFG: Middle frontal gyrus; STG:Superior Temporal gyrus; IFG: Inferior Frontal gyrus; ACC: Anterior Cingulate cortex; SPL: Superior Parietal Lobe; SFG: Superior Frontal gyrus.
doi:10.1371/journal.pone.0107145.t002

in the two groups as far as FC of the four insular subregions with a p<0.02 FDR corrected (Figure 4).

Baseline analysis at T0 confirmed known distinct patterns of connectivity of the four insular subregions. AIlh and AIRh showed significant FC with the ipsilateral inferior frontal gyrus (IFG), the posterior insular cortex, the anterior middle cingulate cortex (aMCC), the ACC, the superior frontal gyrus (SFG), the contralateral anterior and posterior insula. For PIlh and PIrh, FC was found with the putamen bilaterally, the dorsal ACC and
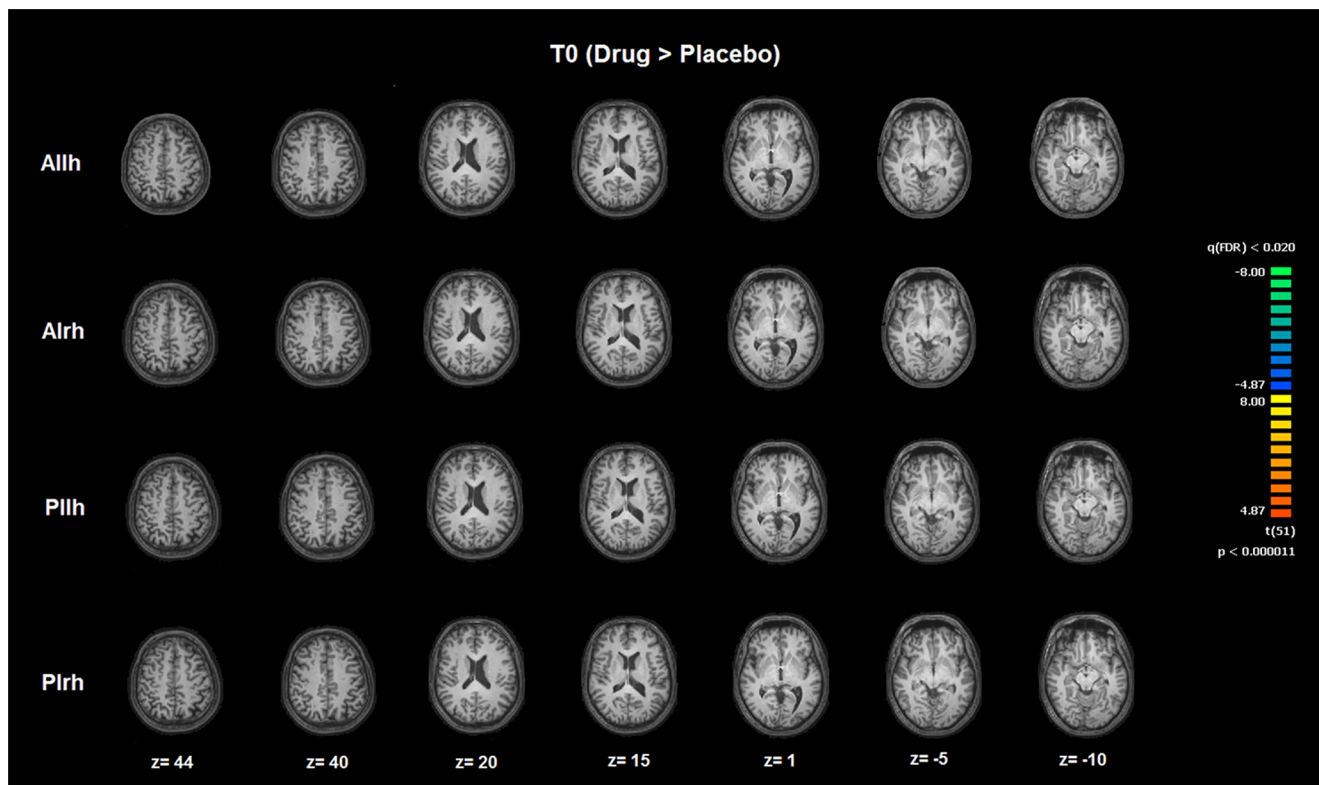

Figure 4. Between-group comparison of the four insula subregions before drug/placebo treatment. Image depicts maps obtained after contrast T0 (Drug>Placebo) for the four subregions of bilateral insulae as assessed with rs-fMRI. Maps are overimposed on a Talairach atlas and in radiological convention (p<0.02 FDR corrected). Differences are assessed by means of a mixed model voxel wise ANOVA with a between-group factor (Drug vs Placebo) and a repeated measure factor (T0 vs. T1) and specific contrast T0 (Drug>Placebo). AIlh = anterior insula left hemisphere; AIrh = anterior insula right hemphere; Pilh = posterior insula left hemisphere; PIrh = posterior insula right hemisphere.
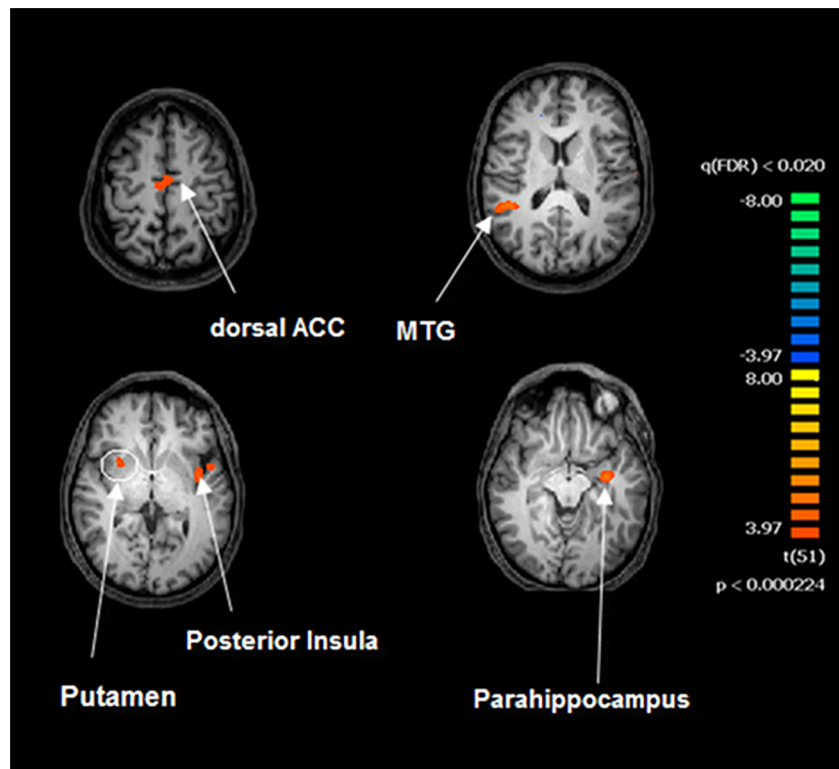doi:10.1371/journal.pone.0107145.g004

Figure 5. Insula functional connectivity patterns after drug/placebo treatment. Image depicts functional connectivity patterns of the four subregions of bilateral insulae as assessed with rs-fMRI. Maps are overimposed on a Talairach atlas and in radiological convention with a statistical significance of p<0.05 Bonferroni corrected. AIlh = anterior insula left hemisphere; AIrh = anterior insula right hemphere; PIlh = posterior insula left hemisphere; PIrh = posterior insula right hemisphere.
doi:10.1371/journal.pone.0107145.g005

the precentral and postcentral gyri as well as with the contralateral anterior and posterior insulae.

At T1, both study groups showed FC maps for AIlh and AIrh that were largely similar to the ones found at T0. AIlh and AIrh showed significant FC with the above listed T0 regions with the addition of the superior temporal gyrus (STG) and the dorsolateral prefrontal cortex (dlPFC). At T1, maps for PIlh and PIrh indicated FC with the contralateral posterior/middle insula, the putamen, the parahyppocampus, the MCC, the precentral/postcentral gyri, and the superior parietal lobule (SPL).

We then performed a comparison of T1 (drug>placebo) versus T0 (drug>placebo) for each seed ROI maps setting significance levels at p<0.02 FDR corrected. AIlh, AIrh and PIlh showed no significant differences. The only significant difference was observed for PIrh. The regions showed, bilaterally, a significant FC increase in the SFG, putamen, and dorsal ACC. A lateralized effect was found in the right hemisphere with significant differences in the middle temporal gyrus whereas significant between-group differences were observed, at T1>T0, for the left posterior insula and left temporal pole up to the parahippocampal region (Figure 3, Table 1).

Discussion

In the present study, we investigated subregional FC effects of modafinil in the insula. Posterior and anterior insular cortices showed differential functional behavior (Figure 2 and 5, Table 2).

In the modafinil group, after drug analysis revealed distinctive FC patterns within nodes of the right posterior insula. After modafinil administration, we found increased FC levels in the

putamen, left parahippocampus, left posterior insula and MCC (Figure 3, Table 2). Our results indicate that the drug does not reorganize FC within sub-regions of the insula but strengthens the region overall connectivity, a phenomenon commonly observed in fMRI studies [44].

In a previous study, we have found that a single dose administration of modafinil does not modify SN activity [14]. However, previous findings indicate that the anterior insula, a major SN hub [15], is activated by modafinil in methamphetamine addicts who were undergoing a reversal learning task [13]. The anterior insula has also been shown to be involved in tasks focused on modulation of fluid reasoning [28], another cognitive function that we have found improved in modafinil treated subjects [14].

Seed-based analysis of functioning of insular subregions offered additional information that could help to reconcile these divergent results.

Our within-group results showed patterns of FC occurring between the anterior insula and frontal regions, the ACC, and the controlateral insula. The posterior insula showed FC with the putamen bilaterally, the dorsal ACC, and the precentral and postcentral gyri as well as with the contralateral anterior and posterior insulae. These FC results are in line with known anatomical connections [35].

Previous rs-fMRI studies have shown that the insula is involved in two distinct neural networks. The first network links the anterior insula to the ACC, the prefrontal and frontal cortex as well as to parietal and temporal regions. The second network links the posterior insular cortex to the middle cingulate, sensorimotor,

premotor, and temporoparietal cortices. This posterior pattern is mainly involved in motor functions such as body orientation, monitoring of the environment and response selection [17,18;45–47].

The two networks communicate with a posterior-anterior modality [18]. Thus, a model can be envisioned by which thalamocortical pathways send a representation of homeostatic information to the posterior insula, thereby generating distinct interoceptive feelings that are projecting onto anterior insula to help in promoting emotional evaluation.

The anterior portion of the insula appears to have a more defined role in the interplay between high cognitive and emotional functions. In addition, compared to the left insula, the right region has a more prominent role in the exploration of the environment and spatial orientation. In particular, the right insula plays a fundamental role in spatial self-orientation and awareness of limb movements in space [48–50].

While many studies have dissected the role of the anterior insula, fewer reports have analyzed functioning of the posterior insula [43].

The right posterior insula appears to be more involved in monitoring the external environment as well as in response selection and action preparation. Several studies indicate that this region is an area of convergence for processing multimodal exteroceptive, interoceptive, vestibular, and auditory stimuli.

In our study, it is conceivable that the drug-dependent increase of FC that we observed between the right insula and putamen can promote enhanced monitoring of internal states aimed at motor planning. The overall nature of the insula-putamen connection lends some support to this hypothesis.

The putamen is a region involved in motivation and reward-related learning [51], the area is in fact important to manage motor actions aimed at obtaining reward [52,53].

The putamen and posterior insula are part of a network that controls decision making processes and impulsivity [54–56]. The dorsal-posterior insula also represents a key region for time encoding [57].

The putamen activity helps in recognizing emotions and bodily states as well as motivation [58,59] and is thought to be driven by increased FC in the MCC, an area involved in goal-directed behavior. The ACC, a region that is functionally and structurally connected to the dorsal striatum, is involved in action planning and motivation. The cingulate cortex is important for social behavior and, supporting this concept, ACC lesions have been shown to lead to akinetic mutism and apathy [60,61].

The hippocampus and insula work together in visuospatial exploration [62]. The parahippocampal regions are also involved in reward processing through activation of the ventral striatum [63–66]. Thus, one can speculate that modafinil may act in the early stages of cognitive processing that are associated with action preparation as well as motivation to act. In that respect, the right posterior insula can sustain motivation by working in synergy with the ACC and putamen along with the intervention of para-hippocampal regions that are responsible for long-term storage of reward-related memories. Preclinical studies have clarified the role of insular orexin receptors in modulating motivation and lend support to our hypothesis as modafinil is a strong orexin receptor agonist [21].

Modafinil-dependent modifications of the right posterior-insula network activity may explain the pro-cognitive effects of the drug. Further research is warrant to evaluate the selective role of the posterior insula as important target for cognitive enhancing drugs.

Supporting Information

Checklist S1 CONSORT 2010 checklist of information included in the modafinil randomised trial.
(PDF)

Protocol S1 Ethic committee approval of the protocol.
(PDF)

Acknowledgments

We thank Alberto Granzotto and Alessandra Mosca for helping with the manuscript preparation.

Author Contributions

Conceived and designed the experiments: NC SLS. Performed the experiments: NC SLS. Analyzed the data: NC AT SLS. Contributed reagents/materials/analysis tools: AT. Contributed to the writing of the manuscript: NC AT SLS.

References

1. Kahbazi M, Ghoreishi A, Rahiminejad F, Mohammadi MR, Kamalipour A, et al. (2009). A randomized double-blind and placebo-controlled trial of modafinil in children and adolescents with attention deficit and hyperactivity disorder. Psychiatry research. 168(3): 234–237.
2. Dawson N, Thompson RJ, McVie A, Thomson DM, Morris BJ, et al. (2012) Modafinil reverses phencyclidine-induced deficits in cognitive flexibility cerebral metabolism and functional brain connectivity. Schizophrenia bulletin 38(3): 457–474.
3. Minzenberg MJ, Watrous AJ, Yoon JH, Ursu S, Carter CS (2008a) Modafinil shifts human locus coeruleus to low-tonic high-phasic activity during functional MRI. Science 322(5908): 1700–1702.
4. Raggi A, Plazzi G, Pennisi G, Tasca D, Ferri R (2011) Cognitive evoked potentials in narcolepsy: a review of the literature. Neuroscience & Biobehavioral Reviews. 35(5): 1144–1153.
5. Nasr S, Wendt B, Steiner K (2006) Absence of mood switch with and tolerance to modafinil: a replication study from a large private practice. J Affect Disord 95111–114.
6. Wisor JP, Nishino S, Sora I, Uhl GH, Mignot E, et al. (2001) Dopaminergic role in stimulant-induced wakefulness. The Journal of Neuroscience 21(5): 1787–1794.
7. Madras BK, Xie Z, Lin Z, Jassen A, Panas H, et al. (2006) Modafinil occupies dopamine and norepinephrine transporters in vivo and modulates the transporters and trace amine activity in vitro. Journal of Pharmacology and Experimental Therapeutics 319(2): 561–569.
8. Volkow ND, Wang GJ, Kollins SH, Wigal TL, Newcorn JH, et al. (2009) Evaluating dopamine reward pathway in ADHD: clinical implications. Jama 302(10): 1084–1091.
9. Turner DC, Robbins TW, Clark L, Aron AR, Dowson J, et al. (2003) Cognitive enhancing effects of modafinil in healthy volunteers. Psychopharmacology 165(3): 260–269.
10. Minzenberg MJ, Carter CS (2007) Modafinil: a review of neurochemical actions and effects on cognition. Neuropsychopharmacology 33(7): 1477–1502.
11. Moldofsky H, Broughton RJ, Hill JD (2000) A randomized trial of the long-term continued efficacy and safety of modafinil in narcolepsy. Sleep medicine 1(2): 109–116.
12. Kollins SH, MacDonald EK, Rush CR (2001) Assessing the abuse potential of methylphenidate in nonhuman and human subjects: a review. Pharmacology Biochemistry and Behavior 68(3): 611–627.
13. Ghahremani DG, Tabibnia G, Monterosso J, Hellemann G, Poldrack RA, et al. (2011) Effect of modafinil on learning and task-related brain activity in methamphetamine-dependent and healthy individuals. Neuropsychopharmacology 36(5): 950–959.
14. Esposito R, Cilli F, Pieramico V, Ferretti A, Macchia A, et al. (2013) Acute Effects of Modafinil on Brain Resting State Networks in Young Healthy Subjects. PloS one 8(7): e69224.
15. Seeley WW, Menon V, Schatzberg AF, Keller J, Glover GH, et al. (2007) Dissociable intrinsic connectivity networks for salience processing and executive control The Journal of neuroscience. 27(9): 2349–2356.
16. Menon V, Uddin LQ (2010) Saliency switching attention and control: a network model of insula function. Brain Structure and Function 214(5–6): 655–667.
17. Taylor KS, Seminowicz DA, Davis KD (2009) Two systems of resting state connectivity between the insula and cingulate cortex. Human brain mapping 30(9):2731–2745.

18. Craig AD (2002) How do you feel? Interoception: the sense of the physiological condition of the body. Nature Reviews Neuroscience 3(8): 655–666.
19. Critchley HD, Wiens S, Rotshtein P, Öhman A, Dolan RJ (2004) Neural systems supporting interoceptive awareness. Nature neuroscience 7(2): 189–195.
20. Seminowicz DA, Davis KD (2007) Pain Enhances Functional Connectivity of a Brain. J Neurophysiol. 97: 3651–3659.
21. Hollander JA, Lu Q, Cameron MD, Kamenecka TM, Kenny PJ (2008) Insular hypocretin transmission regulates nicotine reward. Proceedings of the National Academy of Sciences 105(49): 19480–19485.
22. Corbetta M, Shulman GL (2002) Control of goal-directed and stimulus-driven attention in the brain. Nature reviews neuroscience 3(3): 201–215.
23. Dosenbach NU, Visscher KM, Palmer ED, Miezin FM, Wenger KK, et al. (2006) A core system for the implementation of task sets. Neuron 50(5): 799–812.
24. Fox MD, Raichle ME (2007) Spontaneous fluctuations in brain activity observed with functional magnetic resonance imaging. Nature Reviews Neuroscience 8(9): 700–711.
25. Karnath HO, Baier B (2010) Right insula for our sense of limb ownership and self-awareness of actions. Brain Structure and Function 214(5–6): 411–417.
26. Cauda F, D'Agata F, Sacco K, Duca S, Geminiani G, et al. (2011) Functional connectivity of the insula in the resting brain. Neuroimage 55(1): 8–23.
27. Raven J (2000) The Raven's progressive matrices: change and stability over culture and time. Cognitive psychology 41(1): 1–48.
28. Perfetti B, Saggino A, Ferretti A, Caulo M, Romani GL, et al. (2009) Differential patterns of cortical activation as a function of fluid reasoning complexity. Human brain mapping 30(2): 497–510.
29. Yuan Z, Qin W, Wang D, Jiang T, Zhang Y, et al. (2012) The salience network contributes to an individual's fluid reasoning capacity. Behavioural brain research 229(2): 384–390.
30. Van Den Heuvel MP, Hulshoff Pol HE (2010). Exploring the brain network: a review on resting-state fMRI functional connectivity. European Neuropsychopharmacology, 20(8), 519–534.
31. Biswal B, Zerrin Yetkin F, Haughton VM, Hyde JS (1995) Functional connectivity in the motor cortex of resting human brain using echo-planar mri. Magnetic resonance in medicine 34(4): 537–541.
32. Horwitz B (2003) The elusive concept of brain connectivity. Neuroimage 19(2): 466–470.
33. Birn RM (2007) The behavioral significance of spontaneous fluctuations in brain activity. Neuron 56(1): 8–9.
34. Talairach J, Tournaux P (1988) Co-Planar Stereotaxic Atlas of the Human Brain. Thieme New York, 1988.
35. Augustine JR (1996) Circuitry and functional aspects of the insular lobe in primates including humans. Brain Research Reviews 22(3): 229–244.
36. Fox MD, Snyder AZ, Vincent JL, Corbetta M, Van Essen DC, et al. (2005): The human brain is intrinsically organized into dynamic, anticorrelated functional networks. Proc Natl Acad Sci USA 102:9673–9678.
37. Margulies DS, Kelly AM, Uddin LQ, Biswal BB, Castellanos FX, et al. (2007) Mapping the functional connectivity of anterior cingulate cortex. Neuroimage 37(2): 579–588.
38. Bandettini PA, Bullmore E (2008) Endogenous oscillations and networks in functional magnetic resonance imaging. Human brain mapping 29(7): 737.
39. Napadow V, Dhond R, Conti G, Makris N, Brown EN, et al. (2008) Brain correlates of autonomic modulation: combining heart rate variability with fMRI. Neuroimage 42(1): 169–177.
40. Weissenbacher A, Kasess C, Gerstl F, Lanzenberger R, Moser E, et al. (2009) Correlations and anticorrelations in resting-state functional connectivity MRI: a quantitative comparison of preprocessing strategies. Neuroimage 47(4): 1408–1416.
41. Friston KJ, Holmes AP, Worsley KJ, Poline JP, Frith CD, et al. (1994) Statistical parametric maps in functional imaging: a general linear approach. Human brain mapping 2(4): 189–210.
42. Genovese CR, Lazar NA, Nichols T (2002) Thresholding of statistical maps in functional neuroimaging using the false discovery rate. Neuroimage 15(4): 870–878.
43. Kriegeskorte N, Simmons WK, Bellgowan PS, Baker CI (2009) Circular analysis in systems neuroscience: the dangers of double dipping. Nature neuroscience, 12(5), 535–540.
44. Chang LJ, Yarkoni T, Khaw MW, Sanfey AG (2013) Decoding the role of the insula in human cognition: functional parcellation and large-scale reverse inference. Cerebral Cortex 23(3): 739–749.
45. Flynn FG (1999) Anatomy of the insula functional and clinical correlates Aphasiology 13(1): 55–78.
46. Craig AD (2008) Interoception and emotion: a neuroanatomical perspective In: Lewis M J Haviland-Jones J M Barrett L F (Eds) Handbook of Emotions Guilford Press New York; London pp 272–288.
47. Kurth F, Zilles K, Fox PT, Laird AR, Eickhoff SB (2010) A link between the systems: functional differentiation and integration within the human insula revealed by meta-analysis. Brain Structure and Function 214(5–6): 519–534.
48. Karnath HO, Baier B, Nägele T (2005) Awareness of the functioning of one's own limbs mediated by the insular cortex? The Journal of Neuroscience 25(31): 7134–7138.
49. Fiol ME, Leppik IE, Mireles R, Maxwell R (1988) Ictus emeticus and the insular cortex. Epilepsy research 2(2): 127–131.
50. Schneider RJ, Friedman DP, Mishkin M (1993) A modality-specific somatosensory area within the insula of the rhesus monkey Brain research 621(1): 116–120.
51. Cromwell HC, Hassani OK, Schultz W (2005) Relative reward processing in primate striatum. Experimental Brain Research 162(4): 520–525.
52. Haruno M, Kawato M (2006) Heterarchical reinforcement-learning model for integration of multiple cortico-striatal loops: fMRI examination in stimulus-action-reward association learning. Neural Networks 19(8): 1242–1254.
53. Knutson B, Adams CM, Fong GW, Hommer D (2001) Anticipation of increasing monetary reward selectively recruits nucleus accumbens. Journal of Neuroscience 21(16):1–5.
54. Knutson B, Westdorp A, Kaiser E, Hommer D (2000) FMRI visualization of brain activity during a monetary incentive delay task. Neuroimage 12(1): 20–27.
55. Aron A, Fisher H, Mashek DJ, Strong G, Li H, et al. (2005) Reward motivation and emotion systems associated with early-stage intense romantic love. Journal of neurophysiology 94(1): 327–337.
56. McHugh MJ, Demers CH, Braud J, Briggs R, Adinoff B, et al. (2013) Striatal-insula circuits in cocaine addiction: implications for impulsivity and relapse risk. The American journal of drug and alcohol abuse 39(6): 424–432.
57. Wittmann BC, Tan GC, Lisman JE, Dolan RJ, Düzel E (2013) DAT genotype modulates striatal processing and long-term memory for items associated with reward and punishment. Neuropsychologia 51(11): 2184–2193.
58. Muranishi M, Inokawa H, Yamada H, Ueda Y, Matsumoto N, et al. (2011) Inactivation of the putamen selectively impairs reward history-based action selection. Experimental brain research 209(2): 235–246.
59. Tomer R, Goldstein RZ, Wang GJ, Wong C, Volkow ND (2008) Incentive motivation is associated with striatal dopamine asymmetry. Biological psychology 77(1): 98–101.
60. Damasio AR, Van Hoesen GW (1983) Emotional disturbances associated with focal lesions of the limbic frontal lobe. In Heilman KM and Satz P Editors Guilford Press Neuropsychology of Human Emotion pp 85–110.
61. Devinsky O, Morrell MJ, Vogt BA (1995) Contributions of anterior cingulate cortex to behavior. Brain 118(1): 279–306.
62. Ghaem O, Mellet E, Crivello F, Tzourio N, Mazoyer B, et al. (1997) Mental navigation along memorized routes activates the hippocampus precuneus and insula. Neuroreport 8(3): 739–744.
63. Adcock RA, Thangavel A, Whitfield-Gabrieli S, Knutson B, Gabrieli JD (2006) Reward-motivated learning: mesolimbic activation precedes memory formation. Neuron 50(3): 507–517.
64. Callan DE, Schweighofer N (2008) Positive and negative modulation of word learning by reward anticipation. Human brain mapping 29(2): 237–249.
65. Camara E, Rodriguez-Fornells A, Münte TF (2009) Functional connectivity of reward processing in the brain. Frontiers in Human Neuroscience 2: 19.
66. Lisman JE, Grace AA (2005) The hippocampal-VTA loop: controlling the entry of information into long-term memory. Neuron 46(5): 703–713.